Superconducting Coherence Peak in the Electronic Excitations of a Single-Layer $Bi_2Sr_{1.6}La_{0.4}CuO_{6+\delta}$ Cuprate Superconductor

J. Wei,[1] Y. Zhang,[1] H. W. Ou,[1] B. P. Xie,[1] D. W. Shen,[1] J. F. Zhao,[1] L. X. Yang,[1] M. Arita,[2] K. Shimada,[2] H. Namatame,[2] M. Taniguchi,[2] Y. Yoshida,[3] H. Eisaki,[3] and D. L. Feng[1,*]

[1]*Department of Physics, Surface Physics Laboratory (National Key Laboratory) and Advanced Materials Laboratory, Fudan University, Shanghai 200433, People's Republic of China*

[2]*Hiroshima Synchrotron Radiation Center and Graduate School of Science, Hiroshima University, Hiroshima 739-8526, Japan*

[3]*National Institute of Advanced Industrial Science and Technology (AIST), Tsukuba, Ibaraki 3058568, Japan*

(Received 14 January 2008; published 28 August 2008)

Angle resolved photoemission spectroscopy study is reported on a high quality optimally doped $Bi_2Sr_{1.6}La_{0.4}CuO_{6+\delta}$ high-T_c superconductor. In the antinodal region with a maximal d-wave gap, the symbolic superconducting coherence peak, which has been widely observed in multi-CuO_2-layer cuprate superconductors, is unambiguously observed in a single-layer system. The associated peak-dip separation is just about 19 meV, which is much smaller than its counterparts in multilayered compounds, but correlates with the energy scales of spin excitations in single-layer cuprates.

DOI: 10.1103/PhysRevLett.101.097005 PACS numbers: 74.72.Hs, 71.18.+y, 79.60.Bm

In search of the mechanism of high temperature superconductivity, one central issue is whether there are certain bosons that play the critical mediating role of phonons in a conventional BCS superconductor. So far, signatures of electron-boson interactions have been identified in single particle excitations measured by angle resolved photoemission spectroscopy (ARPES). For example, in the so-called nodal region, where the d-wave superconducting gap diminishes, a characteristic kink [1,2] was discovered in the dispersion of various cuprate superconductors. However, the nature of the corresponding boson, particularly whether it is due to lattice or spin excitations, was intensively debated.

For multi-CuO_2-layer cuprate superconductors, such as $Bi_2Sr_2CaCu_2O_{8+\delta}$ (Bi2212), $Bi_2Sr_2Ca_2Cu_3O_{10+\delta}$ (Bi2223), and $YBa_2Cu_3O_{7-\delta}$ (YBCO) [3–7], a sharp peak emerges out of the normal state broad spectrum when temperature is lowered below the superconducting transition temperature (T_c), forming a so-called "peak-dip-hump" (PDH) structure [see Fig. 4(c) for illustration] in the antinodal region, where the d-wave superconducting gap is at its maximum. This sharp peak, termed the superconducting coherence peak (SCP), contains rich information about superconductivity. Its position reflects the maximal pairing strength, while its intensity grows with decreasing temperature, illustrating the gain of coherence through the development of a superconducting condensate or superfluid [4,8]. The PDH structure has been regarded as evidence for interactions with a bosonic mode [9–16]. However, since this mode energy (~35 meV) coincides with the energy of certain oxygen phonon and spin excitations near (π, π), scenarios based on both kinds of bosons have been put forward.

Recently, SCP has been reported in $La_{2-x}Sr_xCuO_4$ (LSCO) midway between the node and the antinode [17,18]. In this Letter, we report the discovery of the antinodal SCP in an optimally doped single-layer $Bi_2Sr_{1.6}La_{0.4}CuO_{6+\delta}$ (La-Bi2201). We found the peak-dip distance to be about 19 meV, suggesting the possibility of a bosonic mode in La-Bi2201 with a much lower energy than that in Bi2212. This low energy mode seems to correlate with the superconducting gap and the energy scale of spin excitations observed in various single-layer compounds.

La-Bi2201 single crystals were grown with the floating zone technique. Its superior quality is manifested through the very high T_c (34 K) in its class, and a remarkable zero residual resistivity [see Fig. 1(c)] [19,20], which is critical for revealing the intrinsic properties of high-T_c superconductors. The sample is optimally doped, as verified by the linear temperature dependence of resistivity, detailed annealing studies [20], and Fermi surface volume. The ARPES experiments were conducted with 22.5 eV photons and a Scienta-R4000 electron analyzer at beam line 9 of the Hiroshima Synchrotron Radiation Center. The energy resolution was 7 meV. The samples were cleaved in ultrahigh vacuum ($\sim 5 \times 10^{-11}$ mbar) and measured within 10 h. The experiments on Bi2212 and Bi2223 were conducted with 22.7 eV photons and a Scienta-200 electron analyzer at beam line 5-4 of Stanford Synchrotron Radiation Laboratory. The energy resolution was 10 meV. The angular resolution was 0.3° for all experiments.

Photoemission data in the superconducting state of La-Bi2201 are shown in Fig. 1 along eight cuts across the Fermi surface. The data were taken in the Γ-Y quadrant of the Brillouin zone, so that the superstructure band was well separated from the main band. A sharp quasiparticle shows clear dispersion in the nodal region [Figs. 1(a1) and 1(b1)]. The departure from a linear dispersion, or a kink, in the energy range of 40–70 meV could be observed in the first three cuts [Figs. 1(a1), 1(a2), and 1(a3)] The kink diminishes farther away from the nodal region [Fig. 1(a4)], while

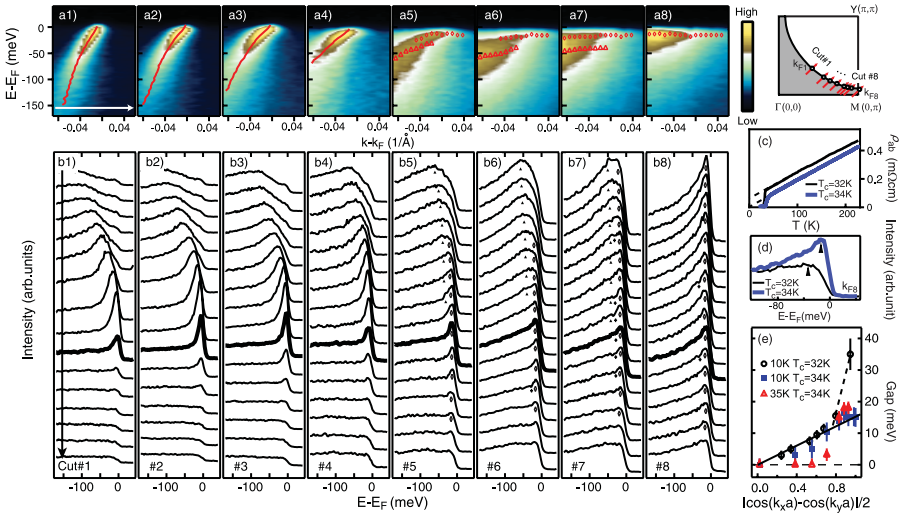

FIG. 1 (color online). Photoemission data of La-Bi2201. (a1)–(a8) Photoemission intensity map along cuts 1–8 across the Fermi surface, as illustrated by arrows in the inset on the upper right. The data were taken at 20 K in the superconducting state. Thick lines in (a1)–(a4) are the dispersions fitted from momentum distribute curves. (b1)–(b8) The corresponding spectra in panels (a1)–(a8). The spectra at various Fermi crossings ($k_{Fi}, i = 1, 2, \ldots, 8$) are in thick curves. The "peak," "dip," and "hump" structures are represented by diamonds, crosses, and triangles, respectively. (c) The resistivity of two La-Bi2201 samples, (d) their corresponding spectrum at k_{F8}, and (e) the momentum dependence of their gaps.

starting from cut 5 in the antinodal region, a feature near the Fermi energy (E_F) gradually becomes quite prominent as indicated by the diamonds in Figs. 1(a5), 1(a6), 1(a7), 1(a8), 1(b5), 1(b6), 1(b7), and 1(b8). Along cuts 5–7, there is also a broad feature at higher binding energy as labeled by the triangles. Though weak, the appearance of such a two-component structure over a broad momentum area clearly proves its robustness against the experimental uncertainties. Eventually, a weak PDH feature is observed in some spectra. In the vicinity of $(\pi, 0)$ [Figs. 1(a8) and 1(b8)], the overall line shape becomes sharper and closer to E_F, so the two components become indistinguishable. This line-shape evolution in Bi2201 is quite different from that in Bi2212. For Bi2212, the kink becomes increasingly pronounced away from the node, and gradually evolves into the PDH in the antinodal region [2,13]. It indicates the subtle differences between single-layer and multilayer cuprates.

The sharp peak in the antinodal region is so delicate that it disappears farther away from the Fermi surface, where the scattering becomes stronger. Therefore, we attribute it to the minimized disorder effects in the current sample [19,20]. As comparison, for another optimally doped La-Bi2201 sample ($T_C = 32$ K) with finite residual resistivity [Fig. 1(c)], its spectrum in the antinodal region is much broader than that of the current sample [Fig. 1(d)]. Consequently, the measured gap at the antinode will be about twice as large, exhibiting the so-called "two-gap" phenomenon as shown in Fig. 1(e) [21]. The momentum distribution of the gap in the $T_C = 32$ K sample consists of two parts: the gap in a large region around the node follows the d-wave form (solid line), and the gap in the antinodal region shows a large deviation. However, for the $T_C = 34$ K sample, its superconducting gap basically follows the d-wave form over the entire Fermi surface. The difference between the two cases occurs when the quasiparticle peak disappears in the $T_C = 32$ K sample near the antinode. As pointed out earlier for LSCO [22], our findings suggest that disorder may play an important role in promoting the two-gap phenomenon. The two-gap–ness for the current sample is more manifested in the temperature dependence: the nodal gap opens only in the superconducting state, whereas there is already a normal state pseudogap of a similar size as the superconducting gap in the antinodal region.

The two-component line shape in the antinodal region alludes to the existence of SCP in La-Bi2201. To further evidence this, the temperature dependences along cuts 1 and 6 are compared in Fig. 2. While the nodal kink structure is temperature independent [Figs. 2(a1), 2(a2), and 2(a3)], a sharp peak along cut 6 gradually emerges out of the normal state broad spectra with decreasing temperature [Fig. 2(b1), 2(b2), and 2(b3)], which is more discernible in the energy distribution curves shown in Figs. 2(c1), 2(c2), and 2(c3). As further illustrated in Figs. 3(a) and 3(b) for two momenta in the antinodal region, the sharp peak

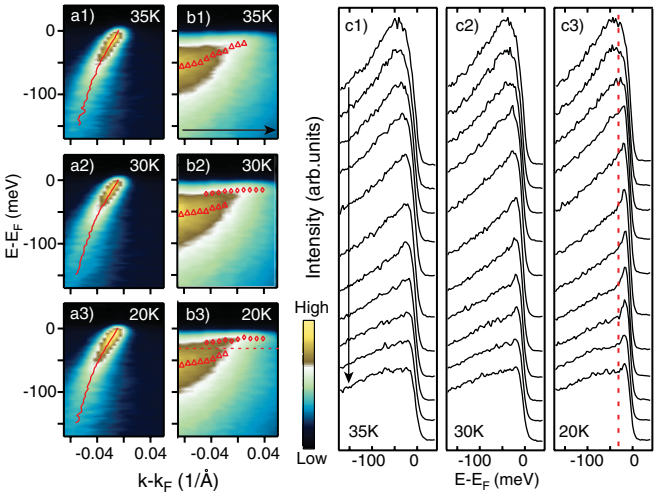

FIG. 2 (color online). Temperature dependence of La-Bi2201 ($T_c = 34$ K) photoemission data along (a1)–(a3) the nodal direction and (b1)–(b3) along cut 6. (c1)–(c3) The energy distribution curves of data in panels (b1)–(b3), respectively. The red dashed line indicates the break between the peaks (diamonds) and humps (triangles).

appears only below T_c, and saturates at low temperatures, just like the temperature dependence of a SCP [4]. We note that the formation of the dip feature is particularly distinct here as well. Moreover, the normal state spectrum at k_{F7} is divided by the resolution convoluted Fermi function of 35 K and then multiplied by that of 10 K, before it is compared with the corresponding 10 K spectrum in Fig. 3 (c). The clear difference shows that the antinodal sharp peaks are not from thermal sharpening. For comparison, following the same procedure, the nodal spectra taken both below and above T_c overlap with each other [Fig. 3(d)]. Therefore, the sharp peak in the antinodal region is the SCP as observed in multilayered cuprates before. It unambiguously rules out scenarios that suggest PDH being caused by bilayer band splitting [23].

The properties of the SCP provide important information about superconductivity. Figure 4(a) shows the associated PDH structures for three momenta near $(\pi, 0)$. Through a phenomenological fitting [4], one could precisely determine the peak position and the separation between the peak and dip, which is about 19 meV at all three momenta. Similarly, the peak-dip structure in Bi2212 ($T_c = 90$ K) also possesses a constant separation of 33 meV at these momenta [Fig. 4(b)] and $(\pi, 0)$ [Fig. 4 (c)]. On the other hand, the peak-dip separations are about 34 meV for Bi2223 ($T_c = 108$ K) and the recently synthesized Bi2212 ($T_c = 96$ K). If one would follow the same analyses as in many previous ARPES studies that the peak-dip separation corresponds to the energy of a bosonic mode [9–16], our Bi2201 data would suggest a bosonic mode of about 19 meV that interacts with the electrons in the antinodal regions. The oxygen B_{1g} phonon, which was argued to be responsible for the PDH in Bi2212 [12,13], is forbidden by symmetry in Bi2201. As shown by Raman scattering [24], phonons with such a low energy are related to the heavy ions, and the oxygen-related phonons are all above 35 meV. Therefore, although electron-phonon interactions can account for the weak temperature dependence of the nodal kink and its presence in heavily overdoped Bi2201 [25], one needs different phonons to explain the antinodal PDH in Bi2212 and Bi2201. On the other hand, the peak-dip separations have an intriguing correlation with the energy scale of spin excitations near (π, π) measured by inelastic neutron scattering on YBCO [26],

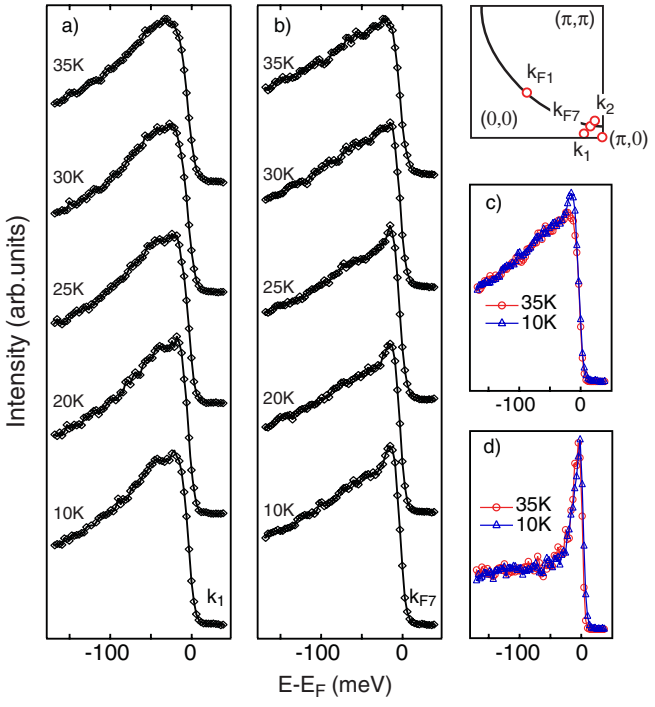

FIG. 3 (color online). Detailed temperature dependence of photoemission data at (a) k_1 and (b) k_{F7}, respectively, in the vicinity of $(\pi, 0)$ as indicated in the inset. (c) and (d) compare the spectra below and above T_c at k_{F7} and k_{F1}, respectively, after removing the temperature broadening effects (see text for details).

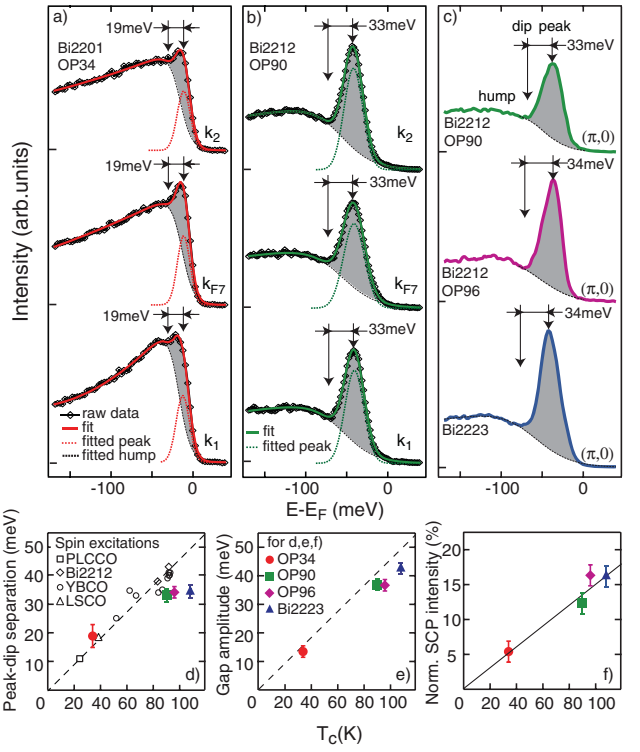

FIG. 4 (color online). SCP near $(\pi, 0)$ for (a) optimally doped single-layer $Bi_2Sr_{1.6}La_{0.4}CuO_{6+\delta}$ ($T_c = 34$ K, OP34) and (b) bilayer $Bi_{2.1}Sr_{1.9}CaCu_2O_{8+\delta}$ ($T_c = 90$ K, OP90) at three momenta (k_1, k_2, and k_{F7} are illustrated in the inset of Fig. 3). (c) Spectra at $(\pi, 0)$ for OP90, $Bi_2Sr_2Ca_{0.92}Y_{0.08}Cu_2O_{8+\delta}$ ($T_c = 96$ K, OP96), and Bi2223 ($T_c = 108$ K). Peak and dip positions are illustrated by the arrows. (d) The peak-dip separation vs T_c for single, bi-, and trilayer bismuth cuprates near optimal doping. The energies of spin excitations near (π, π) for YBCO [26], Bi2212 [27,28], PLCCO [29], and LSCO [30] are plotted for comparison. (e) The superconducting gap amplitude, and (f) the intensity of SCP [shaded region in (a) and (c)] normalized by the total spectral weight over $[E_F - 0.5\,\text{eV}, E_F + 0.1\,\text{eV}]$ as a function of T_c. The SCP is determined from a phenomenological fitting (dashed curves) [4,6]. The dashed lines in (d)–(e) are a fit to the spin excitation energy. The solid line in (f) is a guide to the eye.

Bi2212 [27,28], $Pr_{0.88}LaCe_{0.12}CuO_{4-\delta}$ (PLCCO) [29], and LSCO [30] as a function of T_c [Fig. 4(d)]. Although an inelastic neutron scattering measurement of Bi2201 is currently lacking, the Bi2201 peak-dip separation falls in the dashed line representing the energy scale of the spin excitations [Fig. 4(d)]. Moreover, the temperature dependence of the dip structure correlates with that of the neutron resonance mode [8,16,28]. The weaker dip structure in Bi2201 is consistent with the weaker intensity of the spin excitations observed in low-T_c systems [29,30]. Furthermore, as shown in Fig. 4(e), the superconducting gap amplitude of optimally doped cuprates correlates with T_c and the energy scale of the spin excitations. This resembles the correspondence among the Debye frequency of a phonon, the superconducting gap, and T_c in the BCS theory.

Recent analysis of the Bi2212 scanning tunneling microscopy data [31] suggested that the mode energy could be the separation between the peak and the higher binding energy edge of the dip in the measured density of state, due to the complication of the scattering matrix element and detailed energy and momentum distribution of the states. In this regard, further theoretical analysis is necessary to conclude if the peak-dip separation in the ARPES antinodal spectrum exactly corresponds to the bosonic mode energy. Literally following the scanning tunneling microscopy analysis on antinodal spectra, we obtained a slightly larger mode energy of about 23 meV. From a different perspective, the two-component line shapes, particularly the breaks in dispersions between the peak and hump features [e.g., the dashed lines in Figs. 2(b3) and 2(c3)], are also possible signs of interactions between electrons and bosons. The distance between the peak position at the Fermi momentum and the top of the hump feature gives an upper limit of 25 meV for the mode. These all robustly and self-consistently indicate a low energy mode active in the antinodal region.

Besides the interpretation of electron-boson interactions for PDH, our data seem also to fit in an alternative scenario, where the SCP was considered as the emergence of a coherent quasiparticle out of the broad incoherent background upon superfluid formation [4]. The SCP intensity was found to correlate almost linearly with the superfluid density for Bi2212 [4]. The new La-Bi2201 data fit in a linear relation between relative intensity of the SCP and the optimal T_c [Fig. 4(f)] and thus the superfluid density based on Uemura's plot [32]. Heuristically, for the more stoichiometric $Bi_2Sr_2Ca_{0.92}Y_{0.08}Cu_2O_{8+\delta}$ (OP96) [19,20], its SCP intensity is enhanced, while its gap is similar to that of OP90. Meanwhile, OP96 and Bi2223 have similar SCP intensities, but Bi2223 has a larger gap.

To summarize, we have discovered the PDH in the antinodal region of the single-layer La-Bi2201. The 19 meV peak-dip separation seriously challenges models based on electron-phonon interactions. Meanwhile, this energy scale and temperature dependence intriguingly correlate with the behaviors of spin fluctuations. Our data provide a critical piece to the global picture of the bosonic mode and gap in cuprates, which would help to eventually resolve controversial issues and uncover the "glue" of high-T_c superconductivity.

We gratefully acknowledge helpful discussions with Dr. W. S. Lee, D. H. Lu, Professor Z.-X. Shen, Professor D. H. Lee, Professor T. P. Devereaux , and Professor C. Y. Kim. This work was supported by NSFC, MOST (973 Projects No. 2006CB921300 and No. 2006CB601002), and STCSM of China. The Stanford Synchrotron Radiation Laboratory is operated by the DOE, Office of Basic Energy Science, Divisions of Chemical Sciences and Material Sciences.

*dlfeng@fudan.edu.cn

[1] A. Damascelli, Z. Hussain, and Z. X. Shen, Rev. Mod. Phys. **75**, 473 (2003).
[2] T. Cuk *et al.*, Phys. Status Solidi B **242**, 11 (2005).
[3] D. S. Dessau *et al.*, Phys. Rev. Lett. **66**, 2160 (1991).
[4] D. L. Feng *et al.*, Science **289**, 277 (2000), which also has the details for the phenomenological fitting procedures exploited in Fig. 4.
[5] D. H. Lu *et al.*, Phys. Rev. Lett. **86**, 4370 (2001).
[6] D. L. Feng *et al.*, Phys. Rev. Lett. **88**, 107001 (2002).
[7] H. Matsui *et al.*, Phys. Rev. Lett. **90**, 217002 (2003).
[8] R. H. He *et al.*, Phys. Rev. B **69**, 220502(R) (2004).
[9] J. C. Campuzano *et al.*, Phys. Rev. Lett. **83**, 3709 (1999).
[10] M. R. Norman and H. Ding, Phys. Rev. B **57**, R11089 (1998).
[11] Z. X. Shen and J. R. Schrieffer, Phys. Rev. Lett. **78**, 1771 (1997).
[12] T. P. Devereaux, T. Cuk, Z. X. Shen, and N. Nagaosa, Phys. Rev. Lett. **93**, 117004 (2004).
[13] T. Cuk *et al.*, Phys. Rev. Lett. **93**, 117003 (2004).
[14] Ar. Abanov and A. V. Chubukov, Phys. Rev. Lett. **83**, 1652 (1999).
[15] M. Eschrig and M. R. Norman, Phys. Rev. Lett. **85**, 3261 (2000); **89**, 277005 (2002).
[16] J. F. Zasadzinski *et al.*, Phys. Rev. Lett. **87**, 067005 (2001).
[17] K. Terashima *et al.*, Phys. Rev. Lett. **99**, 017003 (2007).
[18] T. Sato *et al.*, Physica (Amsterdam) **460C–462C**, 864 (2007).
[19] K. Fujita *et al.*, Phys. Rev. Lett. **95**, 097006 (2005).
[20] H. Eisaki *et al.*, Phys. Rev. B **69**, 064512 (2004).
[21] T. Kondo *et al.*, Phys. Rev. Lett. **98**, 267004 (2007).
[22] M. Shi *et al.*, Phys. Rev. Lett. **101**, 047002 (2008).
[23] A. A. Kordyuk *et al.*, Phys. Rev. Lett. **89**, 077003 (2002).
[24] R. Liu *et al.*, Phys. Rev. B **45**, 7392 (1992).
[25] K. Yang *et al.*, Phys. Rev. B **73**, 144507 (2006).
[26] *The Gap Symmetry and Fluctuations in High Temperature Superconductors*, edited by J. Bok *et al.* (Plenum, New York, 1998), p. 37.
[27] H. F. Fong *et al.*, Nature (London) **398**, 588 (1999).
[28] H. He *et al.*, Phys. Rev. Lett. **86**, 1610 (2001).
[29] S. D. Wilson *et al.*, Nature (London) **442**, 59 (2006).
[30] B. Vignolle *et al.*, Nature Phys. **3**, 163 (2007).
[31] J. Lee *et al.*, Nature (London) **442**, 546 (2006).
[32] Y. J. Uemura *et al.*, Physica C (Amsterdam) **282C**, 194 (1997).